

Search for Axionlike and Scalar Particles with the NA64 Experiment

Journal Article

Author(s):

Banerjee, D.; Bernhard, J.; Burtsev, V. E.; Chumakov, A. G.; Cooke, D.; Crivelli, P.; Depero, E.; Dermenev, A. V.; Donskov, S. V.; Dusaev, R. R.; Enik, T.; Charitonidis, N.; Feshchenko, A.; Frolov, V. N.; Gardikiotis, A.; Gerassimov, S. G.; Gninenko, S.N.; Hösgen, M.; Jeckel, M.; Kachanov, V. A.; Molina-Bueno L.; Radics, Balint; Rubbia, A.; Sieber, H.; et al.

Publication date:

2020-08-17

Permanent link:

<https://doi.org/10.3929/ethz-b-000438580>

Rights / license:

[Creative Commons Attribution 4.0 International](#)

Originally published in:

Physical Review Letters 125(8), <https://doi.org/10.1103/PhysRevLett.125.081801>

Search for Axionlike and Scalar Particles with the NA64 Experiment

D. Banerjee,^{4,5} J. Bernhard,⁴ V. E. Burtsev,² A. G. Chumakov,¹⁴ D. Cooke,⁶ P. Crivelli,^{16,†} E. Depero,¹⁶ A. V. Dermenev,⁷ S. V. Donskov,¹¹ R. R. Dusaev,¹³ T. Enik,² N. Charitonidis,⁴ A. Feshchenko,² V. N. Frolov,² A. Gardikiotis,¹⁰ S. G. Gerassimov,^{3,8} S. N. Gninenko,^{7,‡} M. Hösken,¹ M. Jeckel,⁴ V. A. Kachanov,¹¹ A. E. Karneyeu,⁷ G. Kekelidze,² B. Ketzer,¹ D. V. Kirpichnikov,⁷ M. M. Kirsanov,⁷ V. N. Kolosov,¹¹ I. V. Konorov,^{3,8} S. G. Kovalenko,¹² V. A. Kramarenko,^{2,9} L. V. Kravchuk,⁷ N. V. Krasnikov,^{2,7} S. V. Kuleshov,¹² V. E. Lyubovitskij,^{14,15} V. Lysan,² V. A. Matveev,² Yu. V. Mikhailov,¹¹ L. Molina Bueno,¹⁶ D. V. Peshekhonov,² V. A. Polyakov,¹¹ B. Radics,¹⁶ R. Rojas,¹⁵ A. Rubbia,¹⁶ V. D. Samoilenko,¹¹ H. Sieber,¹⁶ D. Shchukin,⁸ V. O. Tikhomirov,⁸ I. Tlisova,⁷ D. A. Tlisov,^{7,*} A. N. Toropin,⁷ A. Yu. Trifonov,¹⁴ B. I. Vasilishin,¹³ G. Vasquez Arenas,¹⁵ P. V. Volkov,^{2,9} V. Yu. Volkov,⁹ and P. Ulloa¹²

(NA64 Collaboration)

¹Universität Bonn, Helmholtz-Institut für Strahlen-und Kernphysik, Bonn 53115, Germany

²Joint Institute for Nuclear Research, Dubna 141980, Russia

³Technische Universität München, Physik Department, Garching 85748, Germany

⁴CERN, European Organization for Nuclear Research, CH-1211 Geneva, Switzerland

⁵University of Illinois at Urbana Champaign, Urbana, Illinois 61801-3080, USA

⁶UCL Department of Physics and Astronomy, University College London, Gower St., London WC1E 6BT, United Kingdom

⁷Institute for Nuclear Research, Moscow 117312, Russia

⁸P.N. Lebedev Physical Institute, Moscow 119991, Russia

⁹Skobeltsyn Institute of Nuclear Physics, Lomonosov Moscow State University, Moscow 119991, Russia

¹⁰Physics Department, University of Patras, 265 04 Patras, Greece

¹¹State Scientific Center of the Russian Federation Institute for High Energy Physics of National Research Center “Kurchatov Institute” (IHEP), Protvino 142281, Russia


¹²Departamento de Ciencias Físicas, Universidad Andres Bello, Sazié 2212, Piso 7, Santiago, Chile

¹³Tomsk Polytechnic University, Tomsk 634050, Russia

¹⁴Tomsk State Pedagogical University, Tomsk 634061, Russia

¹⁵Universidad Técnica Federico Santa María, Valparaíso 2390123, Chile

¹⁶ETH Zürich, Institute for Particle Physics and Astrophysics, CH-8093 Zürich, Switzerland

 (Received 18 May 2020; revised 16 July 2020; accepted 17 July 2020; published 17 August 2020)

We carried out a model-independent search for light scalar (s) and pseudoscalar axionlike (a) particles that couple to two photons by using the high-energy CERN SPS H4 electron beam. The new particles, if they exist, could be produced through the Primakoff effect in interactions of hard bremsstrahlung photons generated by 100 GeV electrons in the NA64 active dump with virtual photons provided by the nuclei of the dump. The $a(s)$ would penetrate the downstream HCAL module, serving as a shield, and would be observed either through their $a(s) \rightarrow \gamma\gamma$ decay in the rest of the HCAL detector, or as events with a large missing energy if the $a(s)$ decays downstream of the HCAL. This method allows for the probing of the $a(s)$ parameter space, including those from generic axion models, inaccessible to previous experiments. No evidence of such processes has been found from the analysis of the data corresponding to 2.84×10^{11} electrons on target, allowing us to set new limits on the $a(s)\gamma\gamma$ -coupling strength for $a(s)$ masses below 55 MeV.

DOI: [10.1103/PhysRevLett.125.081801](https://doi.org/10.1103/PhysRevLett.125.081801)

Published by the American Physical Society under the terms of the [Creative Commons Attribution 4.0 International license](https://creativecommons.org/licenses/by/4.0/). Further distribution of this work must maintain attribution to the author(s) and the published article's title, journal citation, and DOI. Funded by SCOAP³.

Neutral spin-zero scalar (s) or pseudoscalar (a) massive particles are predicted in many extensions of the standard model (SM). The most popular light pseudoscalar, the axion, postulated in [1] to provide a solution to the “strong CP” problem, emerges as a consequence of the breaking of

the Peccei-Quinn (PQ) symmetry [2]. It is now believed that the generic axion has a mass, perhaps much smaller than $m_a \sim O(100)$ keV, which was originally expected [3,4]. The axionlike particles (ALPs), which are pseudo-Nambu-Goldstone bosons, arise in models containing a spontaneously broken PQ symmetry, see, e.g., [5,6], with arbitrary masses and small couplings, making them natural candidates for the mediator of interactions between dark and visible sectors or as candidate for dark matter (DM) themselves. ALPs could also provide a solution to both the electron [7] and muon [8] $g-2$ anomalies [9]. This has motivated worldwide theoretical and experimental efforts towards dark forces and other portals between the visible and dark sectors, see, e.g., [10–21].

The $a - \gamma\gamma$ interaction is given by the Lagrangian

$$L_{\text{int}} = -\frac{1}{4}g_{a\gamma\gamma}F_{\mu\nu}\tilde{F}^{\mu\nu}a, \quad (1)$$

where $g_{a\gamma\gamma}$ is the coupling constant, $F_{\mu\nu}$ is the photon field strength, $\tilde{F}^{\mu\nu} = \frac{1}{2}\epsilon^{\mu\nu\alpha\beta}F_{\alpha\beta}$, and a is the axionlike particle field. For a generic axion, the coupling constant is

$$g_{a\gamma\gamma} = \left[0.203\frac{E}{N} - 0.39\right] \frac{m_a}{\text{GeV}^2} \quad (2)$$

where E and N are the electromagnetic and color anomalies of the axial current associated with the axion [6,22,23]. In grand unified models such as DFSZ [3] and KSVZ [4], $E/N = 8/3$ and $E/N = 0$, respectively, while a broader range of E/N values is possible [6,23]. For the scalar case, an example of an s particle weakly coupled to two photons is the dilaton, which arises in superstring theories and interacts with matter through the trace of the energy-momentum tensor [24], and its two-photon interaction is given by Eq. (1) with the replacement $\tilde{F}^{\mu\nu} \rightarrow F^{\mu\nu}$. Usually, it is assumed that $g_{s\gamma\gamma} = O(M_{\text{Pl}}^{-1})$ and that the dilaton mass $m_s = O(M_{\text{Pl}})$, where M_{Pl} is the Planck mass. However, in some models, see, e.g., [25], the dilaton could be rather

light. Since there are no firm predictions for the coupling $g_{s\gamma\gamma}$ the searches for such particles have become interesting.

Experimental bounds on $g_{a\gamma\gamma}$ for light as in the $\text{eV}/c^2 - \text{MeV}/c^2$ mass range can be obtained from laser experiments [26,27], from experiments studying J/ψ and Υ particles [28], from the NOMAD experiment by using a photon-regeneration method at the CERN SPS neutrino beam [29], and from orthopositronium decays [30]. Limits on ALPs in the $\text{MeV}/c^2 - \text{GeV}/c^2$ mass range have been typically placed by beam-dump experiments or from searches at e^+e^- colliders [6,31], leaving the large area $10^{-2} \lesssim g_{a\gamma\gamma} \lesssim 10^{-5} \text{ GeV}^{-1}$ of the $(g_{a\gamma\gamma}; m_a)$ -parameter space still unprobed. Additionally, since the theory predictions for the coupling, mass scale, and decay modes of ALPs are still quite uncertain, it is crucial to perform independent laboratory tests on the existence of such particles in the mass and coupling strength range discussed above. One possible way to answer these questions is to search for ALPs in a beam dump experiment [6]. However, for the coupling lying in the range $10^{-2} \lesssim g_{a\gamma\gamma} \lesssim 10^{-4} \text{ GeV}^{-1}$ traditional beam dump experiments are not very promising, because, for the masses in the sub- GeV/c^2 region, the a is expected to be a relatively short-lived particle.

In this Letter, we propose and describe a direct search for ALPs with the coupling to two photons from the $(m_a; g_{a\gamma\gamma})$ -parameter space uncovered by previous searches. The application of the obtained results to the $s \rightarrow \gamma\gamma$ decay case is straightforward, see, e.g., [19].

The NA64 detector located at the CERN SPS H4 electron beam [32] is schematically shown in Fig. 1. It consists of a set of beam defining scintillator counters S_{1-4} and veto $V_{1,2}$, a magnetic spectrometer consisting of two dipole magnets (MBPL1,2) and a low-material-budget tracker composed of two upstream Micromegas chambers $\text{MM}_{1,2}$, and four downstream MM_{3-6} stations [33], two straw-tube $\text{ST}_{1,2}$ [34] and $\text{GEM}_{1,2}$ chambers. A synchrotron radiation detector (SRD) is used for the identification of incoming e^- s [35,36] and suppression of the hadron

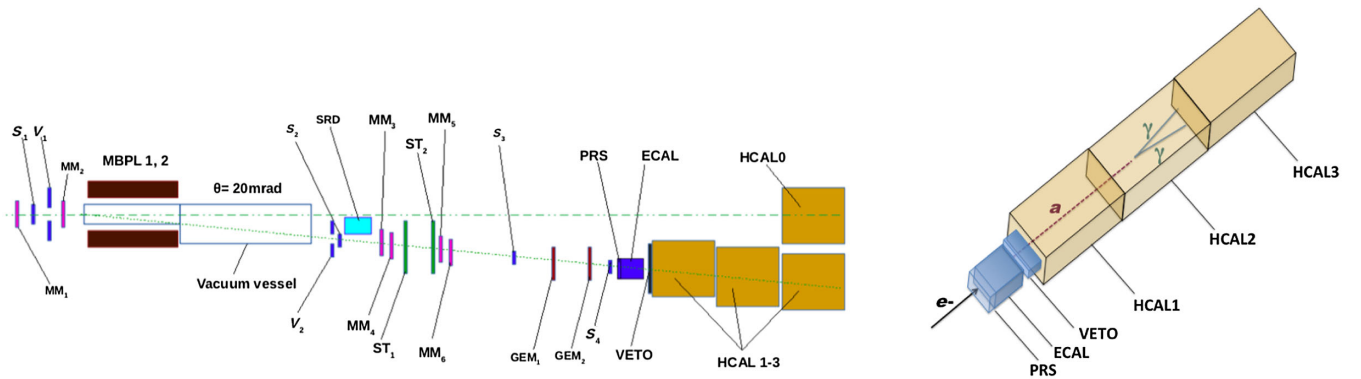


FIG. 1. The left panel illustrates schematic view of the setup to search for the $a \rightarrow \gamma\gamma$ decays of the as produced in the reaction chain $e^-Z \rightarrow e^-Z\gamma; \gamma Z \rightarrow aZ$ induced by 100 GeV e^- s in the active ECAL dump. The right panel shows an example of the $a \rightarrow \gamma\gamma$ decay in the HCAL2 module.

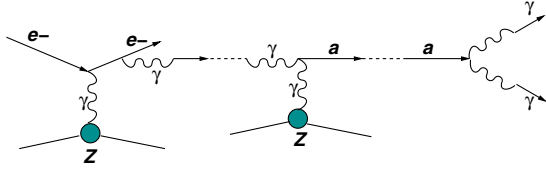


FIG. 2. Illustration of the a production and decay in the reaction of Eq. (3).

contamination in the beam down to the level $\pi/e^- \lesssim 10^{-5}$. An active dump, consisting of a preshower detector (PRS) and an electromagnetic (e-m) calorimeter (ECAL), made of a matrix of 6×6 Shashlik-type modules, is assembled from Pb and Sc plates of $\simeq 40$ radiation lengths (X_0). A large high-efficiency veto counter (VETO) and a massive, hermetic hadronic calorimeter (HCAL) composed of three modules HCAL1-3 complete the setup. Each module is a 3×3 cell matrix with a thickness of $\simeq 7.5$ nuclear interaction lengths. The events from e^- interactions in the PRS and ECAL were collected with the trigger provided by the S_{1-4} requiring also an in-time cluster in the ECAL with the energy $E_{\text{ECAL}} \lesssim 85$ GeV. The detector is described in more detail in Ref. [37].

If ALPs exist, one would expect a flux of such high energy particles from the dump. Both scalars and pseudo-scalars could be produced in the forward direction through the Primakoff effect in interactions of high energy bremsstrahlung photons, generated by 100 GeV electrons in the target, with virtual photons from the electrostatic field of the target nuclei:

$$e^-Z \rightarrow e^-Z\gamma; \quad \gamma Z \rightarrow aZ; \quad a \rightarrow \gamma\gamma, \quad (3)$$

as illustrated in Fig. 2. If the ALP is a relatively long-lived particle, it would penetrate the first downstream HCAL1 module serving as shielding and would be observed in the NA64 detector with two distinctive signatures, either (1) via its decay into 2γ inside the HCAL2 or HCAL3 modules (denoted further as HCAL2,3), or (2) as an event with large missing energy if it decays downstream of the HCAL2,3.

The selection criteria for signal and background samples have been obtained using a GEANT4 [38,39] based Monte Carlo (MC) simulation of the NA64 detector. The code for the simulation of signal events is implemented in the same program according to the general scheme described in [40,41], with the $a \rightarrow \gamma\gamma$ decay width given by $\Gamma_a = g_{a\gamma\gamma}^2 m_a^3 / 64\pi$.

The event from the incoming electron interacting in the dump was required to have the incoming track momentum in the range of 100 ± 3 GeV, the SRD signal within the range of synchrotron radiation emitted by e^- s, a single PRS cluster matched to an isolated ECAL cluster with an energy greater than 0.5 GeV and an ECAL cluster with the shape expected from a single e-m shower [37,40]. As the 2γ opening angle for the $a \rightarrow \gamma\gamma$ decay is very small, it was not

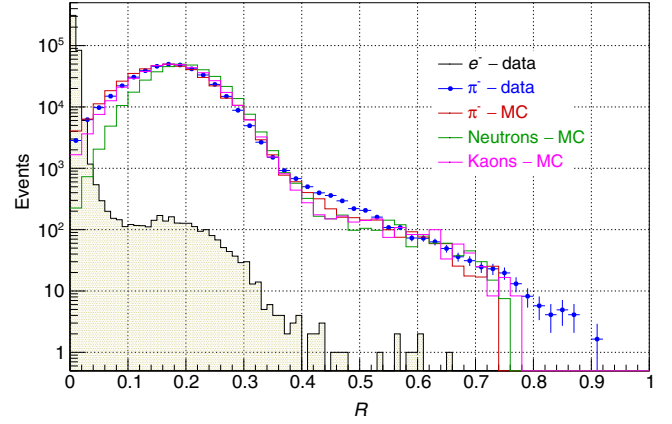


FIG. 3. Distributions of the variable R for the 80 GeV e^- , π^- , K_L^0 , and n events obtained from data during the ECAL and HCAL calibration runs and simulations.

possible to distinguish this decay from a single e-m shower in the HCAL. Therefore, the candidate events with the signature 1 were selected as a single shower in the neutral final state, i.e., no activity in the VETO and the HCAL1, with e-m-like lateral shape, the shower maximum in the HCAL2,3 central cell and the energy deposition $E_{\text{HCAL}} \gtrsim 15$ GeV. This allowed us to reduce background to a small level, while maximizing the a yield by using the cut on the ECAL energy $E_{\text{ECAL}} \lesssim 85$ GeV. For events with the signature 2, we required the ECAL energy to be $E_{\text{ECAL}} \lesssim 50$ GeV and no activity in the VETO and the HCAL. The above event selection criteria, as well as the efficiency corrections, backgrounds and their systematic errors were similar to those used in our searches for the invisible decays of dark photons [37,42].

An additional background suppression for the case 1 was achieved by using the lateral shower shape in the HCAL module. It was characterized by a variable R , defined as $R = (E_{\text{HCAL}} - E_{\text{HCAL}}^c) / (E_{\text{HCAL}})$, where E_{HCAL} , E_{HCAL}^c are the total HCAL energy and the energy deposited in the central cell, respectively. An example of R distributions obtained from data and MC simulations is shown in Fig. 3. As expected, the distribution for e^- s is narrower than for hadrons, and can be employed for effective particle identification. Using the cut $R < 0.06$ rejects $\gtrsim 98\%$ of hadrons, while keeping the signal efficiency $\gtrsim 95\%$.

The search described in this Letter uses data samples of $n_{\text{EOT}} = 2.84 \times 10^{11}$ electrons on target (EOT) collected during the 2016–2018 run period with the beam intensity in the range $\simeq (2 - 9) \times 10^6$ e^-/spill . In Fig. 4(a), the distribution of $\simeq 3 \times 10^4$ events from the reaction $e^-Z \rightarrow$ anything in the $(E_{\text{ECAL}}; E_{\text{HCAL}})$ plane collected with the trigger and by requiring the presence of a beam e^- identified with the SRD tag is shown. Events from the horizontal band with $E_{\text{HCAL}} \simeq 10$ GeV originate from the QED dimuon pair production in the ECAL and were used to cross-check the reliability of the MC simulation and

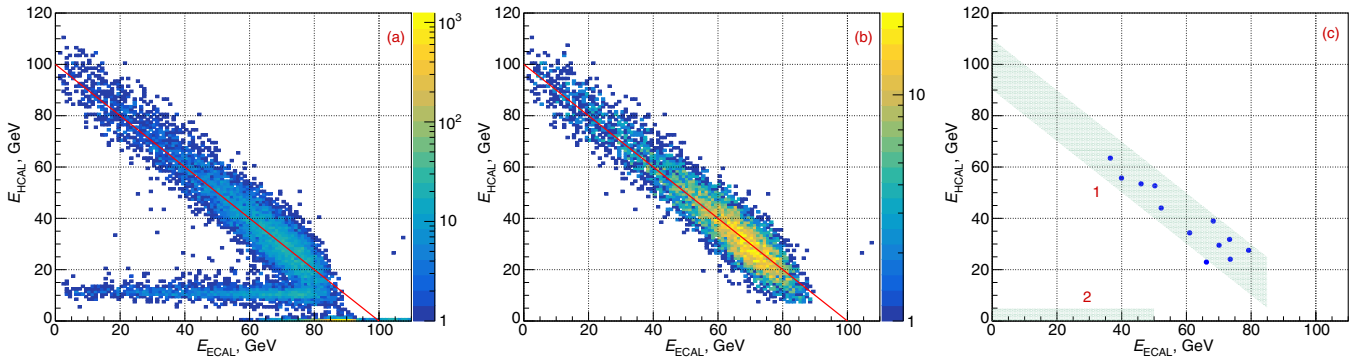


FIG. 4. Panel (a) shows the measured distribution of all events in the $(E_{\text{ECAL}}; E_{\text{HCAL}})$ plane selected at the initial phase of the analysis with the loose cuts. The distribution of pure neutral hadronic secondaries is illustrated in panel (b). The shaded area shown in panel (c) represents the signal boxes 1 and 2 in the $(E_{\text{ECAL}}; E_{\text{HCAL}})$ plane for the signatures 1 and 2, respectively, where no candidates for the signal events were found after applying all selection criteria. The blue dots represent 12 events in the control region $R > 0.06$ from leading neutral hadrons. The size of the signal box 2 is increased by a factor of 5 along the E_{HCAL} axis for the illustration purposes.

background estimate [37]. The further requirement of no activity in the VETO identified a sample of $\simeq 7 \times 10^3$ events shown in Fig. 4(b). This sample corresponds to the neutral hadronic secondaries from electroproduction in the dump with full hadronic energy deposition in the HCAL1 module. The events located mostly along the diagonal satisfy the condition of energy conservation $E_{\text{ECAL}} + E_{\text{HCAL}} \simeq 100$ GeV.

The signal events with the signature 1 are expected to exhibit themselves as an excess of e-m-like events in the $(E_{\text{ECAL}}; E_{\text{HCAL}})$ plane in the signal box 1 [Fig. 4(c)] around the diagonal $E_{\text{ECAL}} + E_{\text{HCAL}} = 100 \pm 10$ GeV satisfying the energy conservation within the energy resolution of the detectors and the cut $R < 0.06$, as shown in Fig. 4(c). By inverting this cut we obtain the control region, where the signal events are almost absent. The signal box 2, $0 \lesssim E_{\text{ECAL}} \lesssim 55$ GeV, $E_{\text{HCAL}} \lesssim 1$ GeV for signal events having a large missing energy is also shown [40,41].

The following processes that may fake the $a \rightarrow \gamma\gamma$ decay in the HCAL2,3 were considered: (1) the production of a leading neutron (n), or (2) a leading K^0 meson in the ECAL by e^- s in the reaction $e^-A \rightarrow n(K^0) + m\pi^0 + X$, that punchthrough the HCAL1 and deposited their energy $E_{n(K^0)} \simeq E_0 - E_{\text{Veto}}$ in the HCAL2,3 either in hadronic interactions with a significant e-m component in the shower, or via $K_S^0 \rightarrow \pi^0\pi^0$ or $K_L^0 \rightarrow 3\pi^0$ decays. The reaction can be accompanied by the production of any number m of π^0 s that decay immediately in the ECAL and a small activity X in the Veto and HCAL1 below the corresponding thresholds $E_{\text{Veto}} \lesssim 0.5MIP$ and $E_{\text{HCAL1}} \lesssim 1$ GeV. (iii) Similar reactions induced by beam π^- and K^- that are not rejected by the SRD. As well as the $\pi^-, K^- \rightarrow e^-\nu$, or $K^- \rightarrow \pi^0 e^-\nu$ decays of poorly detected punchthrough beam π^-, K^- downstream of the HCAL1, or production of a hard bremsstrahlung γ in the downstream part of the HCAL1. (iv) The decays and reactions induced by muons from dimuon pairs produced in the ECAL.

The main background source is expected from the reactions (ii), mostly due to $K_{S,L}^0$ decays in flight. The background was then evaluated by using the simulation combined with the data themselves by two methods. In the first one, we use the sample of $n_n = 7 \times 10^3$ observed neutral events shown in Fig. 4(b). A conservative number of background events originated from leading neutrons and K^0 was defined as $n_b^{n(K^0)} = n_n \times f_{n(K^0)} \times P_{pth}^{n(K^0)} \times P_{em}^{n(K^0)}$, where $f_{n(K^0)}$, $P_{pth}^{n(K^0)}$, and $P_{em}^{n(K^0)}$ are, respectively, the fraction of leading neutrons and kaons in the sample, the probability for $n(K^0)$ to punchthrough the HCAL1, and the probability for the $n(K^0)$ induced shower to be accepted as an e-m one. Using GEANT4 simulations we found $f_{n(K^0)} = 0.2 \pm 0.07(0.18 \pm 0.06)$. The values $P_{pth}^{n(K^0)} \simeq 10^{-3}(4.7 \times 10^{-3})$ were calculated by using measured absorption cross sections from Refs. [43,44]. The values $P_{em}^{n(K^0)} \simeq 5 \times 10^{-3}(1.1 \times 10^{-2})$ were evaluated from the MC distributions of Fig. 3. The systematic errors of 10% and 30% have been assigned to $P_{pth}^{n(K^0)}$ and $P_{em}^{n(K^0)}$ values, respectively, by taking into account the data-MC difference in punchthrough and transverse shapes of showers (see Fig. 3) generated by π s. In the second method we used the number of $n_c = 12$ neutral events observed in the control region, shown in Fig. 4(c). This number was found to be in a good agreement with 9 ± 4 events expected from the sample of neutral events shown in Fig. 4(b). The background then was estimated by taking into account the relative composition of these events which was found to be $\simeq 25\%$ of neutrons and 75% of K^0 s.

All background estimates were then summed up, taking into account the corresponding normalisation factors. These factors were calculated from beam composition, cross sections for the processes listed above, and punchthrough probabilities evaluated directly from the data and MC simulations. The total number of expected candidate

TABLE I. Expected background for 2.84×10^{11} EOT.

Background source	Background, n_b
Leading neutrons	0.02 ± 0.008
Leading K^0 interactions and decays	0.14 ± 0.045
Beam π , K charge exchange and decays	0.006 ± 0.002
Dimuons	<0.001
Total n_b	0.17 ± 0.046

events after applying the selection criteria are given in Table I for each background component. The total background of 0.17 ± 0.046 events, where statistical and systematic errors were added in quadrature, estimated with the first method was found to agree with the second estimate resulting in 0.19 ± 0.07 events. For the signature 2, the total background in the data sample was estimated to be 0.53 ± 0.17 events, as described in detail in Ref. [42].

After determining all the selection criteria and background levels, we unblinded the signal boxes. No event in the signal boxes shown in Fig. 4(c) were found, allowing us to obtain the m_a -dependent upper limits on the coupling strength $g_{a\gamma\gamma}$. The exclusion limits were calculated by employing the multibin limit setting technique in the ROOSTATS package [45] with the modified frequentist approach, using the profile likelihood as a test statistic [46–48]. The combined 90% confidence level (C.L.) limits on the coupling strength $g_{a\gamma\gamma}$ were obtained from the corresponding limit for the expected number of signal events, n_a , which is given by the sum:

$$n_a = \sum_{i=1}^2 \varepsilon_a^i n_a^i(g_{a\gamma\gamma}, m_a), \quad (4)$$

where ε_a^i is the signal efficiency and $n_a^i(g_{a\gamma\gamma}, m_a)$ is the number of the a decays for the signature i . The a yield from the reaction chain (3) was obtained with the calculations described in Ref. [49] assigning $\lesssim 10\%$ systematic uncertainty due to different form-factor parametrizations [50,51]. An additional uncertainty of $\simeq 10\%$ was accounted for the data-MC difference for the dimuon yield [37,52]. The signal detection efficiency for each signature in (4) was evaluated by using signal MC and was found slightly m_a dependent. For instance, for the signature 1 and $m_a \simeq 10$ MeV, the ε_a^1 and its systematic error was determined from the product of efficiencies accounting for the geometrical acceptance (0.97 ± 0.02), the primary track ($\simeq 0.83 \pm 0.04$), SRD ($\gtrsim 0.95 \pm 0.03$), ECAL (0.95 ± 0.03), VETO (0.94 ± 0.04), HCAL1 (0.94 ± 0.04), and HCAL2,3 (0.97 ± 0.02) signal event detection. The signal efficiency loss $\lesssim 7\%$ due to pileup was taken into account using reconstructed dimuon events [37]. The VETO and HCAL1 efficiencies were defined as a fraction of events below the corresponding energy thresholds with the main uncertainty estimated to be $\lesssim 4\%$ for the signal events,

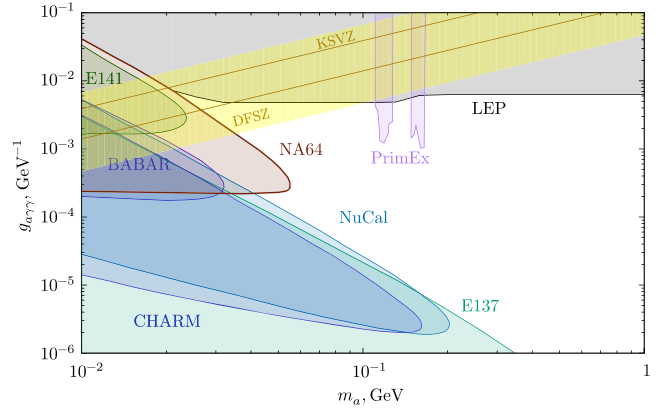


FIG. 5. The NA64 90% C.L. exclusion region for ALPs coupling predominantly to photons in the $(m_a, g_{a\gamma\gamma})$ plane as a function of the (pseudo)scalar mass m_a derived from the present analysis. The yellow band represents the parameter space for the benchmark DFSZ [3] and KSVZ [4] models extended with a broader range of E/N values [6,23]. Constraints from the BABAR [31], E137 [53], E141 [54,55], LEP [56], and PrimEx [57] experiments, as well as limits from CHARM [58] and NuCal [59], updated in Ref. [60] are also shown. For more limits from indirect searches and proposed measurements; see, e.g., Refs. [11–13].

which is caused by the pileup effect from penetrating hadrons. The trigger efficiency was found to be 0.95 with a small uncertainty of 2%. The total signal efficiency ε_a varied from 0.51 ± 0.09 to 0.48 ± 0.08 for the a mass range of 10–50 MeV. The total systematic uncertainty on n_a calculated by adding all errors in quadrature did not exceed 20% for both signatures. The attenuation of the a flux due to interactions in the HCAL1 was found to be negligible. The combined signal region excluded in the $(m_a, g_{a\gamma\gamma})$ plane at 90% C.L. is shown in Fig. 5 together with the results of other experiments. Our limits are valid for both scalar and pseudoscalar cases and exclude the region in the coupling range $2 \times 10^{-4} \lesssim g_{a\gamma\gamma} \lesssim 5 \times 10^{-2} \text{ GeV}^{-1}$ for masses $m_a \lesssim 55$ MeV.

We gratefully acknowledge the support of the CERN management and staff and the technical staff of the participating institutions for their vital contributions. We would like to thank M. W. Krasny for providing us with Ref. [54] and useful comments, B. Döbrich for providing information on the E141 and updated CHARM and NuCal exclusion curves, and G. Lanfranchi for valuable discussions. This work was supported by the Helmholtz-Institut für Strahlen- und Kernphysik (HISKP), University of Bonn, the Carl Zeiss Foundation Grant No. 0653-2.8/581/2, and Verbundprojekt-05A17VTA-CRESST-XENON (Germany), Joint Institute for Nuclear Research (JINR) (Dubna), the Ministry of Science and Higher Education (MSHE) in the frame of the Agreement No. 075-15-2020-718 ID No. RFMEFI61320X0098, TPU Competitiveness

Enhancement Program and RAS (Russia), ETH Zurich and SNSF Grants No. 169133, No. 186181, and No. 186158 (Switzerland), and FONDECYT Grants No. 1191103, No. 190845, and No. 3170852, UTFSM PI M 18 13, Agencia Nacional Investigacion y Desarrollo (ANID), Programa de Investigacion Asociativa (PIA) AFB180002 (Chile).

*Deceased

†Corresponding author.

Paolo.Crivelli@cern.ch

‡Corresponding author.

Sergei.Gninenko@cern.ch

- [1] S. Weinberg, *Phys. Rev. Lett.* **40**, 223 (1978); F. Wilczek, *Phys. Rev. Lett.* **40**, 279 (1978).
- [2] R. D. Peccei and H. R. Quinn, *Phys. Rev. Lett.* **38**, 1440 (1977).
- [3] M. Dine, W. Fischler, and M. Srednicki, *Phys. Lett. B* **104**, 199 (1981); A. Zhitnitski, *Yad. Fiz.* **31**, 497 (1980) [*Sov. J. Nucl. Phys.* **31**, 260 (1980)].
- [4] J. E. Kim, *Phys. Rev. Lett.* **43**, 103 (1979); M. Schifman, A. Vainstein, and V. Zakharov, *Nucl. Phys.* **166**, 493 (1981).
- [5] N. V. Krasnikov, V. A. Matveev, and A. N. Tavkhelidze, *Sov. J. Part. Nucl.* **12**, 38 (1981); J. E. Kim, *Phys. Rep.* **150**, 1 (1987); H. Y. Cheng, *Phys. Rep.* **158**, 1 (1988); G. Raffelt, *Phys. Rep.* **198**, 1 (1990).
- [6] M. Tanabashi *et al.* (Particle Data Group), *Phys. Rev. D* **98**, 030001 (2018).
- [7] R. H. Parker, C. Yu. W. Zhong, B. Estey, and H. Müller, *Science* **360**, 191 (2018).
- [8] G. W. Bennett *et al.* (Muon g-2 Collaboration), *Phys. Rev. D* **73**, 072003 (2006).
- [9] H. Davoudiasl and W. J. Marciano, *Phys. Rev. D* **98**, 075011 (2018); C. Shi, Y. L. Du, S. S. Xu, X. J. Liu, and H. S. Zong, *Phys. Rev. D* **93**, 036006 (2016); W. J. Marciano, A. Masiero, P. Paradisi, and M. Passera, *Phys. Rev. D* **94**, 115033 (2016); F. Abu-Ajamieh, *Adv. High Energy Phys.* **2020**, 1751534 (2020).
- [10] R. Essig *et al.*, arXiv:1311.0029.
- [11] J. Alexander *et al.*, arXiv:1608.08632.
- [12] M. Battaglieri *et al.*, arXiv:1707.04591.
- [13] J. Beacham *et al.*, *J. Phys. G* **47**, 010501 (2020).
- [14] R. Alemany *et al.*, arXiv:1902.00260.
- [15] A. Berlin, N. Blinov, G. Krnjaic, P. Schuster, and N. Toro, *Phys. Rev. D* **99**, 075001 (2019).
- [16] J. L. Feng, I. Galon, F. Kling, and S. Trojanowski, *Phys. Rev. D* **98**, 055021 (2018).
- [17] B. Döbrich, J. Jaeckel, F. Kahlhoefer, A. Ringwald, and K. Schmidt-Hoberg, *J. High Energy Phys.* **02** (2016) 018.
- [18] M. Bauer, M. Heiles, M. Neubert, and A. Thamm, *Eur. Phys. J. C* **79**, 74 (2019).
- [19] J. Jaeckel and M. Spannowsky, *Phys. Lett. B* **753**, 482 (2016).
- [20] S. N. Gninenko, N. V. Krasnikov, and V. A. Matveev, arXiv:2003.07257.
- [21] D. V. Kirpichnikov, V. E. Lyubovitskij, and A. S. Zhevlakov, arXiv:2002.07496.
- [22] G. G. di Cortona, E. Hardy, J. Pardo Vega, and G. Villadoro, *J. High Energy Phys.* **01** (2016) 034.
- [23] J. E. Kim, *Phys. Rev. D* **58**, 055006 (1998); L. Di Luzio, F. Mescia, and E. Nardi, *Phys. Rev. Lett.* **118**, 031801 (2017).
- [24] P. Horava and E. Witten, *Nucl. Phys.* **B460**, 506 (1996); **B475**, 94 (1996).
- [25] N. Arkani-Hamed, S. Dimopoulos, and G. Dvali, *Phys. Lett. B* **429**, 263 (1998); I. Antoniadis, N. Arkani-Hamed, S. Dimopoulos, and G. Dvali, *Phys. Lett. B* **436**, 257 (1998).
- [26] G. Russo *et al.*, *Z. Phys. C* **56**, 505 (1992).
- [27] R. Cameron *et al.*, *Phys. Rev. D* **47**, 3707 (1993).
- [28] M. S. Alam *et al.*, *Phys. Rev. D* **27**, 1665 (1983); N. J. Baker, H. A. Gordon, D. M. Lazarus, V. A. Polychronakos, P. Rehak *et al.*, *Phys. Rev. Lett.* **59**, 2832 (1987).
- [29] P. Astier *et al.* (NOMAD Collaboration), *Phys. Lett. B* **479**, 371 (2000).
- [30] U. Amaldi, G. Carboni, B. Jonson, and J. Thun, *Phys. Lett.* **153B**, 444 (1985); S. Orito, K. Yoshimura, T. Haga, M. Minowa, and M. Tsuchiaki, *Phys. Rev. Lett.* **63**, 597 (1989); M. V. Akopian, G. S. Atoyian, S. N. Gninenko, and V. V. Sukhov, *Phys. Lett. B* **272**, 443 (1991); S. N. Gninenko, Yu. M. Klubakov, A. A. Poblaguev, and V. E. Postoev, *Phys. Lett. B* **237**, 287 (1990); T. Maeno, M. Fujikawa, J. Kataoka, Y. Nishihara, S. Orito, K. Shigekuni, and Y. Watanabe, *Phys. Lett. B* **351**, 574 (1995); S. Asai, S. Orito, K. Yoshimura, and T. Haga, *Phys. Rev. Lett.* **66**, 2440 (1991).
- [31] M. J. Dolan, T. Ferber, C. Hearty, F. Kahlhoefer, and K. Schmidt-Hoberg, *J. High Energy Phys.* **12** (2017) 094.
- [32] See, for example, <http://sba.web.cern.ch/sba/>.
- [33] D. Banerjee, P. Crivelli, and A. Rubbia, *Adv. High Energy Phys.* **2015**, 1 (2015).
- [34] V. Yu. Volkov, P. V. Volkov, T. L. Enik, G. D. Kekelidze, V. A. Kramarenko, V. M. Lysan, D. V. Peshekhonov, A. A. Solin, and A. V. Solin, *Phys. Part. Nucl. Lett.* **16**, 847 (2019).
- [35] S. N. Gninenko, *Phys. Rev. D* **89**, 075008 (2014).
- [36] E. Depero *et al.*, *Nucl. Instrum. Methods Phys. Res., Sect. A* **866**, 196 (2017).
- [37] D. Banerjee, V. E. Burtsev, A. G. Chumakov, D. Cooke, P. Crivelli *et al.* (NA64 Collaboration), *Phys. Rev. D* **97**, 072002 (2018).
- [38] S. Agostinelli *et al.* (GEANT4 Collaboration), *Nucl. Instrum. Methods Phys. Res., Sect. A* **506**, 250 (2003).
- [39] J. Allison *et al.*, *IEEE Trans. Nucl. Sci.* **53**, 270 (2006).
- [40] S. N. Gninenko, N. V. Krasnikov, M. M. Kirsanov, and D. V. Kirpichnikov, *Phys. Rev. D* **94**, 095025 (2016).
- [41] S. N. Gninenko, D. V. Kirpichnikov, M. M. Kirsanov, and N. V. Krasnikov, *Phys. Lett. B* **782**, 406 (2018).
- [42] D. Banerjee *et al.* (NA64 Collaboration), *Phys. Rev. Lett.* **123**, 121801 (2019).
- [43] T. J. Roberts, H. R. Gustafson, L. W. Jones, M. J. Longo, and M. R. Whalley, *Nucl. Phys.* **B159**, 56 (1979).
- [44] A. S. Carroll *et al.*, *Phys. Lett.* **80B**, 319 (1979).
- [45] I. Antcheva *et al.*, *Comput. Phys. Commun.* **180**, 2499 (2009).
- [46] T. Junk, *Nucl. Instrum. Methods Phys. Res., Sect. A* **434**, 435 (1999).

- [47] G. Cowan, K. Cranmer, E. Gross, and O. Vitells, *Eur. Phys. J. C* **71**, 1 (2011).
- [48] A. L. Read, *J. Phys. G* **28**, 2693 (2002).
- [49] D. V. Kirpichnikov, R. R. Dusaev, and M. M. Kirsanov, [arXiv:2004.04469](https://arxiv.org/abs/2004.04469).
- [50] Y. Z. Chen, Y. A. Luo, L. Li, H. Shen, and X. Q. Li, *Commun. Theor. Phys.* **55**, 1059 (2011).
- [51] Y. Tsai, *Phys. Rev. D* **34**, 1326 (1986).
- [52] D. Banerjee, V. Burtsev, D. Cooke, P. Crivelli, E. Depero (NA64 Collaboration), *Phys. Rev. Lett.* **118**, 011802 (2017).
- [53] J. D. Bjorken, S. Ecklund, W. R. Nelson, A. Abashian, C. Church, B. Lu, L. W. Mo, T. A. Nunamaker, and P. Rassmann, *Phys. Rev. D* **38**, 3375 (1988).
- [54] M. W. Krasny *et al.* (E141 Collaboration), Preprint University of Rochester, UR-1029, 1987; The E141 limits in $(g_{\gamma\gamma}; m_a)$ plane were obtained in Ref. [55].
- [55] B. Döbrich, *CERN Proc.* **1**, 253 (2018).
- [56] G. Abbiendi *et al.* (OPAL Collaboration), *Eur. Phys. J. C* **26**, 331 (2003).
- [57] D. Aloni, C. Fanelli, Y. Soreq, and M. Williams, *Phys. Rev. Lett.* **123**, 071801 (2019).
- [58] F. Bergsma *et al.* (CHARM Collaboration), *Phys. Lett. B* **157**, 458 (1985).
- [59] J. Blümlein *et al.*, *Z. Phys. C* **51**, 341 (1991).
- [60] B. Döbrich, J. Jaeckel, and T. Spadaro, *J. High Energy Phys.* **05** (2019) 213.